

Investigating maximal steered coherence under the common impacts of reservoir and noise

Ling-Ling Xing(邢玲玲), Huan Yang(杨欢), and Gang Zhang(张刚)

Citation: Chin. Phys. B, 2025, 34 (**5**): 050304. DOI: 10.1088/1674-1056/adbbc2
Journal homepage: http://cpb.iphy.ac.cn; http://iopscience.iop.org/cpb

What follows is a list of articles you may be interested in

Model-free prediction of chaotic dynamics with parameter-aware reservoir computing

Jianmin Guo(郭建敏), Yao Du(杜瑶), Haibo Luo(罗海波), Xuan Wang(王晅), Yizhen Yu(于一真), and Xingang Wang(王新刚)

Chin. Phys. B, 2025, 34 (**4**): 040505. DOI: 10.1088/1674-1056/adb733

Phase-matching enhanced quantum phase and amplitude estimation of a two-level system in a squeezed reservoir

Yan-Ling Li(李艳玲), Cai-Hong Liao(廖彩红), and Xing Xiao(肖兴)

Chin. Phys. B, 2025, 34 (**1**): 010307. DOI: 10.1088/1674-1056/ad8f9e

Enhancing quantum temporal steering via frequency modulation

Mengkai Wu(吴孟凯) and Weiwen Cheng(程维文)

Chin. Phys. B, 2024, 33 (**5**): 050306. DOI: 10.1088/1674-1056/ad2505

Visualizing and witnessing first-order coherence, Bell nonlocality and purity by using a quantum steering ellipsoid in the non-inertial frame

Huan Yang(杨欢), Ling-Ling Xing(邢玲玲), Ming-Ming Du(杜明明), Min Kong(孔敏), Gang Zhang(张刚), and Liu Ye(叶柳)

Chin. Phys. B, 2023, 32 (**10**): 100305. DOI: 10.1088/1674-1056/acb762

Characterizing the dynamics of quantum discord under phase damping with POVM measurements

Jiang Feng-Jian (蒋峰建), Ye Jian-Feng (叶剑锋), Yan Xin-Hu (闫新虎), Lü Hai-Jiang (吕海江)

Chin. Phys. B, 2015, 24 (**10**): 100304. DOI: 10.1088/1674-1056/24/10/100304

Investigating maximal steered coherence under the common impacts of reservoir and noise

Ling-Ling Xing(邢玲玲), Huan Yang(杨欢)[†], and Gang Zhang(张刚)[‡]

School of Electrical and Photoelectronic Engineering, West Anhui University, Lu'an 237012, *China*

(Received 11 January 2025; revised manuscript received 20 February 2025; accepted manuscript online 3 March 2025)

Maximal steered coherence (MSC) is a noteworthy resource measure in the field of quantum information, and it is defined under the framework of coherence measure and the formalism of quantum steering ellipsoids (QSEs). Here, we explore the MSC of a two-qubit X state under the common influences of reservoir and noise. The results disclose that the introduction of auxiliary qubits can give rise to enhancement of the MSC in both the strong and weak coupling regimes. Moreover, more auxiliary qubits can decrease the oscillation period of the MSC, and also suppress the oscillation amplitude of the MSC in the strong coupling regime. In contrast, the increases in auxiliary qubits result in the oscillation of the MSC for the setting of the initially weak coupling regime. Of particular interest is that the improvement effects of more auxiliary qubits on the MSC in the initially weak coupling regime are significantly stronger than that in the initially strong coupling regime.

Keywords: maximal steered coherence, quantum steering ellipsoid, reservoir, noise

PACS: 03.67.–a, 03.65.Yz, 03.65.Ud

DOI: 10.1088/1674-1056/adbbc2 **CSTR:** 32038.14.CPB.adbbc2

1. Introduction

Quantum resource is an important topic and direction in quantum information, and it expands our understanding of non-classical phenomena in the quantum world. Quantum coherence is a promising quantum resource, and it can achieve quantification for the coherence of quantum systems.[1–3] Quantum coherence has found seminal applications in various quantum information processing tasks, such as quantum channel discrimination,[4] quantum algorithms,[5] quantum phase transitions,[6,7] quantum metrology,[8,9] quantum biology and quantum thermodynamics.[10,11] One can use the l_1 norm of coherence,[1] the skew information of coherence,[12,13] the robustness of coherence[14–16] and the relative entropy of coherence[1] to measure quantum coherence of a quantum state. On the basis of these avenues for quantifying quantum coherence, some novel quantum non-localities have been revealed, such as the nonlocal advantage of quantum coherence.[17–23] Among these quantification methods for quantum coherence, the l_1 norm of coherence of a single-qubit system has significant geometric properties, and it provides a nontrivial tool for intuitively ascertaining quantum systems.[24]

If a visual description of a two-qubit system can be achieved, it will provide a valuable approach for intuitively exploring various quantum resources. However, this is not a simple task. As an illustration, one must use 15 state parameters to depict a two-qubit state, and this number of parameters leads to enormous difficulties for visual display of a two-qubit state. Of particular note is that the creative construction of a quantum steering ellipsoid (QSE)[25] can act as an introduction to the visual investigations of two-qubit states and quantum resources. More specifically, if one uses all possible local operations to measure one qubit of a bipartite state, the QSE (in the Bloch sphere) consists of all Bloch vectors of steered states for the other qubit. A QSE provides a visual and faithful formulation for an arbitrary two-qubit system. The theory of QSEs has been gradually enriched and improved, including the requirement for QSEs to describe a two-qubit state.[26] Using QSEs there have been many remarkable achievements in visualizing quantum resources and quantum non-localities, for instance entanglement,[25–27] discord,[25,28–30] quantum phase transitions,[31] Einstein–Podolsky–Rosen steering[32–37] and Bell nonlocality.[38]

Notably, Hu *et al.* proposed the fusion of a QSE and quantum coherence, and introduced steered coherence and maximum steered coherence (MSC).[39] The relevant observations concerning MSC were then implemented in different systems.[40–44] A variety of environments or noises seriously hinder the performance of various quantum information tasks in different systems. A reservoir system is an important physical model for probing non-classical phenomena.[42,45–58] Nevertheless, improvements in MSC under the common impacts of reservoir and noise are still not apparent. Relevant investigations could shed new light on understanding quantum resources, reservoirs and noise environments. Motivated by this,

[†]Corresponding author. E-mail: hyang@wxc.edu.cn

[‡]Corresponding author. E-mail: zhanggang@wxc.edu.cn

© 2025 Chinese Physical Society and IOP Publishing Ltd. All rights, including for text and data mining, AI training, and similar technologies, are reserved.

we ascertain the MSC of a two-qubit X state (because the characterization of many physical contexts is for two-qubit X states[23,44,59]) under the common influences of reservoir and generalized amplitude damping (GAD) noise, and strengthen MSC in both strong and weak coupling regimes by introducing auxiliary qubits to the reservoir. The purpose of simultaneously considering both reservoir and noise (the topic of this paper) is as follows. There are two qubits, one belonging to Alice and the other to Bob. Bob's qubit is affected by GAD noise; however, GAD noise cannot affect Alice's qubit. To protect the MSC, Alice's qubit is coupled to a reservoir containing many auxiliary qubits. This physical image can further uncover the effectiveness and capability of auxiliary qubits in the reservoir for improving MSC under additional noise.

The theoretical model and MSC are concisely introduced in Section 2. In Section 3, our attention is directed to characterize the QSE and MSC of a system, and investigate and augment the MSC under the common influences of reservoir and GAD noise, including the strong and weak coupling regimes. Finally, a summary of our results is provided in Section 4.

2. Theoretical model and MSC

There is a common zero-temperature reservoir, and a system of N identical qubits (two-level atoms, with the N identical qubits decoupled from each other) is immersed in the reservoir. The Hamiltonian of the system is ($\hbar = 1$)[42]

$$H = \sum_{j=1}^{N} \wp_0 \sigma_j^+ \sigma_j^- + \sum_k \chi_k d_k^\dagger d_k + \sum_{j=1}^{N} \sum_k (\omega_k^j \sigma_j^+ d_k + \omega_k^{j*} \sigma_j^- d_k^\dagger). \tag{1}$$

The lowering (raising) operator of the jth qubit is σ_j^- (σ_j^+). The coupling strength of the kth field mode (it has frequency χ_k) and the jth atom is ω_k^j. $\wp_0$ is the transition frequency between the excited state and the ground state. The annihilation (creation) operator of the kth field mode is d_k ($d_k^\dagger$). One assumes $\omega_k^j = \Upsilon_k/\sqrt{N}$ and defines

$$|\Psi_l\rangle = \frac{1}{\sqrt{N}} \sum_{m=0}^{N-1} \exp\left(\frac{2\mathrm{i}\pi ml}{N}\right) |m+1\rangle, \quad (l = 0, 1, \ldots, N-1). \tag{2}$$

The total Hamiltonian is[42]

$$H = \sum_{j=0}^{N-1} \wp_0 |\Psi_j\rangle\langle\Psi_j| + \sum_k \chi_k d_k^\dagger d_k + \sum_k (\Upsilon_k |\Psi_0\rangle\langle 0| d_k + \Upsilon_k^* |0\rangle\langle\Psi_0| d_k^\dagger). \tag{3}$$

Consider the initial state of a system of N two-level atoms,

$$|\psi(0)\rangle = c_0(0)|0\rangle_S|0\rangle_E + \sum_{j=0}^{N-1} Q_j(0)|\Psi_j\rangle_S|0\rangle_E. \tag{4}$$

$|0\rangle_S$ ($|0\rangle_E$) is the ground state of the system (the vacuum state of the field). The time-evolved state is[42]

$$|\psi(t)\rangle = c_0(t)|0\rangle_S|0\rangle_E + \sum_{j=0}^{N-1} Q_j(t)|\Psi_j\rangle_S|0\rangle_E + \sum_k R_k(t)|0\rangle_S|1_k\rangle_E. \tag{5}$$

$R_k(t)$ and $Q_j(t)$ are time-dependent coefficients. $|1_k\rangle_E$ is the state of the reservoir with single excitation in the kth field mode

$$\frac{\mathrm{d}Q_0(t)}{\mathrm{d}t} = -\mathrm{i}\wp_0 Q_0(t) - \mathrm{i}\sum_k \Upsilon_k R_k(t), \tag{6}$$

$$\frac{\mathrm{d}R_k(t)}{\mathrm{d}t} = -\mathrm{i}\chi_k R_k(t) - \mathrm{i}\Upsilon_k^* Q_0(t), \tag{7}$$

$$\frac{\mathrm{d}Q_j(t)}{\mathrm{d}t} = -\mathrm{i}\wp_0 Q_j, \quad \tilde{Q}_j(t) = \mathrm{e}^{\mathrm{i}\wp_0 t} Q_j(t),$$

$$\tilde{R}_k(t) = \mathrm{e}^{\mathrm{i}\chi_k t} R_k(t),$$

$$\frac{\mathrm{d}\tilde{Q}_0(t)}{\mathrm{d}t} = -\mathrm{i}\sum_k \Upsilon_k \mathrm{e}^{\mathrm{i}(\wp_0-\chi_k)t} \tilde{R}_k(t), \tag{8}$$

$$\frac{\mathrm{d}\tilde{R}_k(t)}{\mathrm{d}t} = -\mathrm{i}\Upsilon_k^* \mathrm{e}^{-\mathrm{i}(\wp_0-\chi_k)t} \tilde{Q}_0(t), \tag{9}$$

and $\tilde{Q}_j(t) = \tilde{Q}_j(0)$. Integrating Eq. (9) and substituting it into Eq. (8), we get[42]

$$\frac{\mathrm{d}\tilde{Q}_0(t)}{\mathrm{d}t} = -\int_0^t f(t-t')\tilde{Q}_0(t')\mathrm{d}t' \tag{10}$$

with

$$f(t-t') = \int_{-\infty}^{\infty} \mathrm{d}\chi\, \aleph(\chi) \mathrm{e}^{\mathrm{i}(\wp_0-\chi)(t-t')} \tag{11}$$

and

$$\aleph(\chi) = \sum_k |\Upsilon_k|^2 \delta(\chi - \chi_k) = N\sum_k |\omega_k|^2 \delta(\chi - \chi_k) = NJ(\chi) \tag{12}$$

is the spectral density of the reservoir. Considering the Lorentzian spectral density of the reservoir

$$J(\chi) = \frac{1}{2\pi} \frac{\gamma_0 \lambda}{(\chi - \chi_c)^2 + \lambda^2}. \tag{13}$$

The spectral width is λ, the central frequency of the reservoir is χ_c, and the coupling strength is γ_0. $\gamma_0 > \lambda/(2N)$ is the strong coupling regime (the non-Markovian dynamic) and $\gamma_0 < \lambda/(2N)$ is the weak coupling regime (the Markovian dynamic).[60] If the qubits are in the exact resonance condition with the cavity field ($\chi_c = \wp_0$), the exact solution of $Q_0(t)$ is[42]

$$\tilde{Q}_0(t) = \mathrm{e}^{-\lambda t/2}\left[\cosh\left(\frac{Rt}{2}\right) + \frac{\lambda}{R}\sinh\left(\frac{Rt}{2}\right)\right]\tilde{Q}_0(0) \tag{14}$$

with $R=\sqrt{\lambda^2-2N\gamma_0\lambda}$. One can rewrite the $|\psi(t)\rangle$ of Eq. (5) as[42]

$$|\psi(t)\rangle = c_0(t)|0\rangle_{\rm S}|0\rangle_{\rm E}+\sum_{j=0}^{N-1}\xi_j(t)|j+1\rangle_{\rm S}|0\rangle_{\rm E} +\sum_k R_k(t)|0\rangle_{\rm S}|1_k\rangle_{\rm E} \tag{15}$$

with

$$\xi_j(t)=\frac{1}{\sqrt{N}}\sum_{m=0}^{N-1}\exp\left(\frac{2{\rm i}\pi mj}{N}\right)Q_m(t). \tag{16}$$

Two qubits (two-level atoms) are collectively shared by Alice (A) and Bob (B). Only Bob's atom suffers from the local environment, and the Alice's atom does not interact with the reservoir. Then, one adds some auxiliary atoms to the common reservoir. The first atom is deemed as the system of Bob (it can be excited), and the remaining atoms are treated as the auxiliary qubits (in their ground states). If the initial probability amplitudes $\xi_1(0)=\xi_2(0)=\cdots=\xi_{N-1}(0)=0$, the probability amplitude is $\xi_0(t)=X(t)\xi_0(0)$ with[42]

$$X(t) = {\rm e}^{-{\rm i}\wp_0 t}\left\{\frac{N-1}{N} +\frac{{\rm e}^{-\lambda t/2}}{N}\left[\cosh\left(\frac{Rt}{2}\right)+\frac{\lambda}{R}\sinh\left(\frac{Rt}{2}\right)\right]\right\}. \tag{17}$$

Bob'system is

$$\rho^{\rm B}(t)=\begin{pmatrix}\rho^{\rm B}_{00}(0)+\rho^{\rm B}_{11}(0)(1-p(t)) & \rho^{\rm B}_{01}(0)\sqrt{p(t)}\\ \rho^{\rm B}_{10}(0)\sqrt{p(t)} & \rho^{\rm B}_{11}(0)p(t)\end{pmatrix} \tag{18}$$

with $p(t)=|X(t)|^2$.

Next, we aim to introduce the QSE and MSC. For a bipartite state $\rho_{\rm AB}$, if one uses all local measurements to measure Alice's qubit, Bob's QSE ($\varepsilon_{\rm B}$) is composed by the Bloch vectors of Bob's steered states. The center of $\varepsilon_{\rm B}$ is[25]

$$c_{\rm B}=\frac{(\boldsymbol{b}-\boldsymbol{T}^{\rm T}\boldsymbol{a})}{1-a^2}, \tag{19}$$

and ellipsoid matrix is

$$Q_{\rm B}=\frac{(\boldsymbol{T}^{\rm T}-\boldsymbol{b}\boldsymbol{a}^{\rm T})}{1-a^2}(\boldsymbol{I}+\frac{\boldsymbol{a}\boldsymbol{a}^{\rm T}}{1-a^2})(\boldsymbol{T}-\boldsymbol{a}\boldsymbol{b}^{\rm T}). \tag{20}$$

The orientations of the QSE axes correspond to the eigenvectors of $Q_{\rm B}$, and the squares of the QSE semiaxis lengths correspond to the eigenvalues of $Q_{\rm B}$. $\boldsymbol{a}$ and $\boldsymbol{b}$ are the Bloch vectors of Alice and Bob, respectively. $\boldsymbol{T}$ is the spin correlation matrix of $\rho_{\rm AB}$.

Assuming $\{|\varpi_i\rangle\}$ are the eigenstates of $\rho_{\rm B}$, if one implements a positive operator-valued measure (POVM) on Alice, and obtains an outcome g (the measure operator is $\boldsymbol{G}$), Bob's state is steered to $\rho^G_{\rm B}={\rm tr}_{\rm A}(\boldsymbol{G}\otimes\boldsymbol{I}\rho_{\rm AB})/{\rm tr}(\boldsymbol{G}\otimes\boldsymbol{I}\rho_{\rm AB})$. In the basis $\{|\varpi_i\rangle\}$, the quantum coherence of $\rho^G_{\rm B}$ is

$$C(\rho^G_{\rm B},\{|\varpi_i\rangle\}) = \frac{1}{{\rm tr}(\boldsymbol{G}\otimes\boldsymbol{I}\rho_{\rm AB})} \times\sum_{i\neq j}\left|\langle\varpi_i|{\rm tr}_{\rm A}(\boldsymbol{G}\otimes\boldsymbol{I}\rho_{\rm AB})\left|\varpi_j\right\rangle\right|. \tag{21}$$

For all possible POVM operators $\boldsymbol{G}$, the MSC is the maximum of $C(\rho^G_{\rm B},\{|\varpi_i\rangle\})$[39,44]

$$\mathrm{MSC}(\rho^G_{\rm B}) = \max_{G\in\mathrm{POVM}}\left[\frac{1}{{\rm tr}(\boldsymbol{G}\otimes\boldsymbol{I}\rho_{\rm AB})} \times\sum_{i\neq j}\left|\langle\varpi_i|{\rm tr}_{\rm A}(\boldsymbol{G}\otimes\boldsymbol{I}\rho_{\rm AB})\left|\varpi_j\right\rangle\right|\right]. \tag{22}$$

$\{|\varpi_i\rangle\}$ is not uniquely defined for a degenerate $\rho^G_{\rm B}$, and thus the MSC is

$$\mathrm{MSC}(\rho^G_{\rm B}) = \inf_{\{|\varpi_i\rangle\}}\left\{\max_{G\in\mathrm{POVM}}\left[\frac{1}{{\rm tr}(\boldsymbol{G}\otimes\boldsymbol{I}\rho_{\rm AB})} \times\sum_{i\neq j}\left|\langle\varpi_i|{\rm tr}_{\rm A}(\boldsymbol{G}\otimes\boldsymbol{I}\rho_{\rm AB})\left|\varpi_j\right\rangle\right|\right]\right\}. \tag{23}$$

More specifically, the MSC is the maximal perpendicular distance from the surface of $\varepsilon_{\rm B}$ to the reference basis. For an X state, if the direction of the reference basis is consistent with an axis of $\varepsilon_{\rm B}$ (if the direction of the reference basis is not consistent with the semiaxes of $\varepsilon_{\rm B}$), then the MSC is the longest semiaxis of the other two semiaxes (the MSC is the longest semiaxis of $\varepsilon_{\rm B}$).

3. Exploring the MSC under the common influences of reservoir and GAD noise

Here, Alice and Bob share a two-qubit X state

$$\rho^X_{\rm AB}=\frac{1}{4}\left(\boldsymbol{I}\otimes\boldsymbol{I}+\boldsymbol{r}\cdot\boldsymbol{\sigma}\otimes\boldsymbol{I}+\boldsymbol{I}\otimes\boldsymbol{s}\cdot\boldsymbol{\sigma}+\sum_{i=1}^{3}\tau_i\sigma_i\otimes\sigma_i\right), \tag{24}$$

$$\tau_i={\rm Tr}(\rho^X_{\rm AB}\sigma_i\otimes\sigma_i),\quad (i=1,2,3) \tag{25}$$

with $\boldsymbol{s}=(0,0,s)$, $\boldsymbol{r}=(0,0,r)$, and $\sigma_n=(\sigma_1,\sigma_2,\sigma_3)$. We consider the GAD channel[61] as noise, and the Kraus operators are

$$\Re_1=\sqrt{q}\begin{pmatrix}1 & 0\\ 0 & \sqrt{1-m}\end{pmatrix},\quad \Re_2=\sqrt{q}\begin{pmatrix}0 & \sqrt{m}\\ 0 & 0\end{pmatrix},$$
$$\Re_3=\sqrt{1-q}\begin{pmatrix}\sqrt{1-m} & 0\\ 0 & 1\end{pmatrix},\quad \Re_4=\sqrt{1-q}\begin{pmatrix}0 & 0\\ \sqrt{m} & 0\end{pmatrix}. \tag{26}$$

The decay strength $m=1-{\rm e}^{-\Gamma t'}$ is related to the storage time t' of the atom and the relaxation rate Γ. The decay probability $q=1/(1+{\rm e}^{-\hbar\omega/k_{\rm B}T})$, with $0.5\leq q\leq 1$. In this paper, the GAD noise only disturbs Bob's atom, and the reservoir mentioned above (together with $N-1$ auxiliary qubits) directly affects Alice's atom. In the following investigations, we fix t (corresponding to the reservoir) and change m, and this actually corresponds to changing t'.[61–64] $N=1$ means the absence of an auxiliary qubit. The physical motivation for the

coupling between GAD noise and Bob's atom is to achieve the result that the information of system flows from the system to the environment (namely, the coupling can accelerate the degeneration of quantum resource). The physical purpose of the coupling between $N-1$ auxiliary qubits and Alice's atom is that auxiliary qubits can bring on the backflow of information from the reservoir to the system. This scheme can effectively improve quantum resource. Under the common impacts of reservoir and noise, the final state is

$$\begin{aligned}\rho_{\text{final}} = {} & \aleph_{11}|00\rangle\langle 00| + \aleph_{22}|01\rangle\langle 01| + \aleph_{33}|10\rangle\langle 10| \\ & + \aleph_{44}|11\rangle\langle 11| + \aleph_{23}|01\rangle\langle 10| + \aleph_{32}|10\rangle\langle 01| \\ & + \aleph_{14}|00\rangle\langle 11| + \aleph_{41}|11\rangle\langle 00|, \end{aligned} \tag{27}$$

$$\begin{aligned}\aleph_{11} = {} & \frac{1}{4}\{m[4q-2-2s-p(\tau_3-1+2q+r-2qr-s)] \\ & + p(\tau_3-1+r-s)+2(1+s)\}, \end{aligned} \tag{28}$$

$$\begin{aligned}\aleph_{22} = {} & \frac{1}{4}\{2-2s+p(r+s-\tau_3-1) \\ & + m[2-4q+p(\tau_3-1+2q+r-2qr-s)+2s]\}, \end{aligned} \tag{29}$$

$$\aleph_{33} = \frac{1}{4}p\{\tau_3(m-1)-[1+m(2q-1)](r-1)+s-ms]\}, \tag{30}$$

$$\aleph_{44} = \frac{1}{4}p\{\tau_3(1-m)+[m(2q-1)-1](r-1)-s+ms]\}, \tag{31}$$

$$\aleph_{23} = \aleph_{32} = \frac{1}{4}(\tau_1+\tau_2)\sqrt{p(1-m)}, \tag{32}$$

$$\aleph_{14} = \aleph_{41} = \frac{1}{4}(\tau_1-\tau_2)\sqrt{p(1-m)}. \tag{33}$$

The QSE of Bob is

$$\varepsilon_{\text{B}} = \left\{ \begin{pmatrix} 0 \\ 0 \\ \wp_{\text{B}} \end{pmatrix} + \begin{pmatrix} \Im_x x_1 \\ \Im_y x_2 \\ \Im_z x_3 \end{pmatrix} | x \le 1 \right\}. \tag{34}$$

The x, y and z semiaxis lengths of ε_{B} are

$$\Im_x = \frac{\tau_1\sqrt{p(1-m)}}{\sqrt{p(1-r)[2+p(r-1)]}}, \tag{35}$$

$$\Im_y = \frac{\tau_2\sqrt{p(1-m)}}{\sqrt{p(1-r)[2+p(r-1)]}}, \tag{36}$$

$$\Im_z = \frac{(m-1)(\tau_3-rs)}{(r-1)[2+p(r-1)]}. \tag{37}$$

The ellipsoid's center in the z axis is

$$\wp_{\text{B}} = \frac{\tau_3(1-m)[1+p(r-1)]+m(2q-1)[2+p(r-1)](r-1)+(m-1)s[2+p(r-1)-r]}{(r-1)[2+p(r-1)]}. \tag{38}$$

In our paper, the eigenvector of ρ_{B} of the system (reference basis) along the z-axis, and thus the MSC of the steered states of Bob, is

$$\text{MSC}(\rho_{\text{B}}^{\text{M}}) = \text{Max}\{\Im_x, \Im_y\}. \tag{39}$$

To begin with, we focus our attention on investigating and controlling the MSC in the situation when $(\lambda = 5, \gamma_0 = 30)$ (i.e., we consider the initial scenario in which the system is in the strong coupling regime in the absence of auxiliary qubits, and it is treated as an initially strong coupling regime). In order to investigate the MSC under the common impacts of reservoir and noise, figure 1 reveals the dependence of MSC on decay strength m. To ensure that the initial state is an entangled state, we choose $(r = 0.3, s = 0.2)$ or $(r = -0.3, s = -0.2)$, and also make τ_1, τ_2, and τ_3 satisfy $\tau_2 = -\tau_1\tau_3$ (i.e., the state preparation and measurement choice condition[65]) in all figures. Our results reveal that MSC decreases with increasing m. Of particular interest is that the MSC can be obviously strengthened by coupling five auxiliary qubits ($N = 6$) with the reservoir in Fig. 1(a). However, more auxiliary qubits (from $N = 6$ to $N = 26$) cannot give rise to conspicuous enhancement of the MSC, and one can only use five auxiliary qubits to improve the MSC under the common impacts of reservoir and noise. If one sets $(r = -0.3, s = -0.2)$ in Fig. 1(b), the improvement effects of five auxiliary qubits on the MSC in Fig. 1(b) are significantly better than in Fig. 1(a). In comparison with five auxiliary qubits ($N = 6$), the increase in MSC is not significant when 25 auxiliary qubits are introduced ($N = 26$) in Fig. 1(b). It can be concluded that MSC is very sensitive to auxiliary qubits, and only a few auxiliary qubits can achieve conspicuous improvement in MSC in the strong coupling regime of $(\lambda = 5, \gamma_0 = 30)$.

We now use Fig. 2 to ascertain the dependence of MSC on decay probability q by adding auxiliary qubits in the strong coupling regime. As seen from Fig. 2(a) the MSC is invariant (namely, MSC is frozen at a fixed value) as q grows. By coupling more auxiliary qubits ($N = 6$ or $N = 26$) with the reservoir, the MSC can be frozen at a higher value in Fig. 2, whether $(r = 0.3, s = 0.2)$ or $(r = -0.3, s = -0.2)$. Similarly, in order to achieve a remarkable enhancement in the MSC, one only needs a few auxiliary qubits (e.g., only five auxiliary qubits are needed).

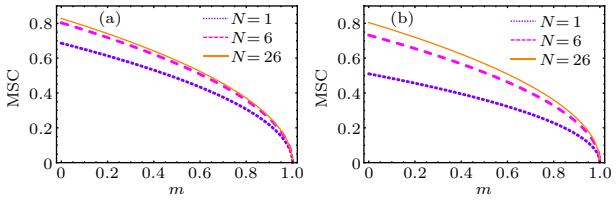


Fig. 1. MSC as a function of m: (a) $r = 0.3$ and $s = 0.2$, (b) $r = -0.3$ and $s = -0.2$. For all plots, $\tau_1 = 0.8$, $\tau_2 = -0.4$, $\tau_3 = 0.5$, $q = 0.6$, $t = 0.3$, $\lambda = 5$ and $\gamma_0 = 30$.

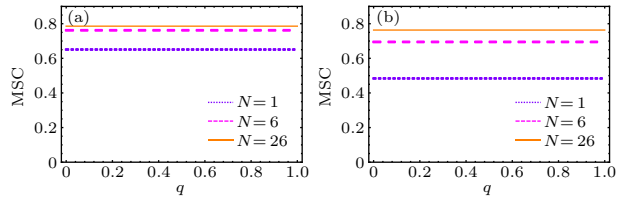


Fig. 2. MSC as a function of q: (a) $r = 0.3$ and $s = 0.2$, (b) $r = -0.3$ and $s = -0.2$. For all plots, $\tau_1 = 0.8$, $\tau_2 = -0.4$, $\tau_3 = 0.5$, $m = 0.1$, $t = 0.3$, $\lambda = 5$ and $\gamma_0 = 30$.

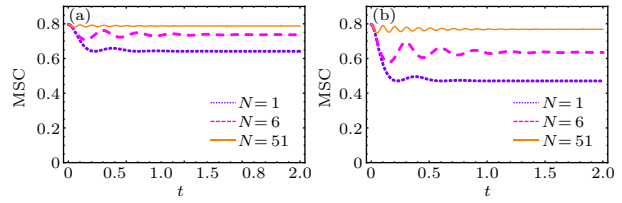


Fig. 3. MSC as a function of t: (a) $r = 0.3$ and $s = 0.2$, (b) $r = -0.3$ and $s = -0.2$. For all plots, $\tau_1 = 0.8$, $\tau_2 = -0.4$, $\tau_3 = 0.5$, $m = 0.1$, $q = 0.6$, $\lambda = 5$ and $\gamma_0 = 30$.

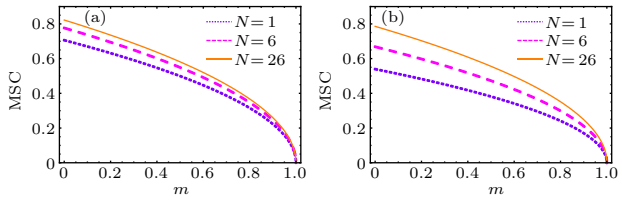


Fig. 4. MSC as a function of m: (a) $r = 0.3$ and $s = 0.2$, (b) $r = -0.3$ and $s = -0.2$. For all plots, $\tau_1 = 0.8$, $\tau_2 = -0.4$, $\tau_3 = 0.5$, $q = 0.6$, $t = 0.3$, $\lambda = 30$ and $\gamma_0 = 5$.

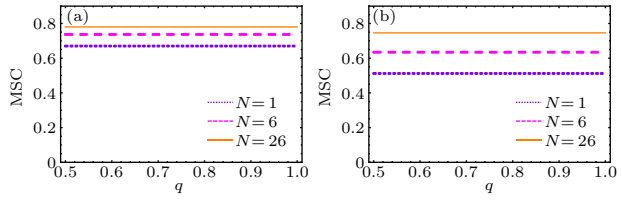


Fig. 5. MSC as a function of q: (a) $r = 0.3$ and $s = 0.2$, (b) $r = -0.3$ and $s = -0.2$. For all plots, $\tau_1 = 0.8$, $\tau_2 = -0.4$, $\tau_3 = 0.5$, $m = 0.1$, $t = 0.3$, $\lambda = 30$ and $\gamma_0 = 5$.

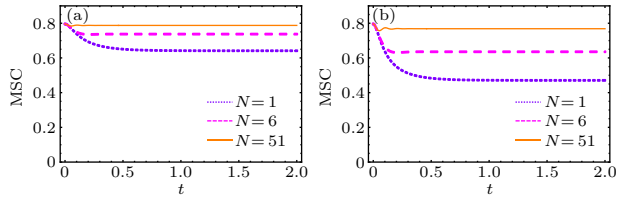


Fig. 6. MSC as a function of t: (a) $r = 0.3$ and $s = 0.2$, (b) $r = -0.3$ and $s = -0.2$. For all plots, $\tau_1 = 0.8$, $\tau_2 = -0.4$, $\tau_3 = 0.5$, $m = 0.1$, $q = 0.6$, $\lambda = 30$ and $\gamma_0 = 5$.

In Fig. 3 we aim to reveal the influence of auxiliary qubits on MSC under different values of t. In the absence of auxiliary qubits ($N = 1$), MSC speedily declines with increasing t (as demonstrated in Fig. 3(a)). Thereafter, MSC is frozen at a fixed value after a brief oscillation process. The introduction of five auxiliary qubits is responsible for augmentation of the MSC, and also gives rise to a reduction of the oscillation period of the MSC. If one uses 50 auxiliary qubits ($N = 51$) in the reservoir, the MSC can be immediately frozen at a higher value, and 50 auxiliary qubits can also effectively suppress the oscillation amplitude of the MSC. In the scenario when $r = -0.3$ and $s = -0.2$ (Fig. 3(b)), the improvement effects of auxiliary qubits on the MSC are more effective than in Fig. 3(a). It is worthwhile emphasizing that more auxiliary qubits can decrease the oscillation period of the MSC in Fig. 3(b); however, the effect of auxiliary qubits in suppressing the oscillation amplitude of the MSC is worse than in Fig. 3(a). Even if 50 auxiliary qubits are introduced, the oscillation amplitude of the MSC in Fig. 3(b) is larger than that in Fig. 3(a) (as the orange curves show in Fig. 3).

Finally, our attention is directed to improving MSC in the case of $\lambda = 30$ and $\gamma_0 = 5$ (namely, we consider the initial situation in which the system is in the weak coupling regime in the absence of auxiliary qubits, and is deemed as an initially weak coupling regime) via auxiliary qubits. It turns out that one can use 5 or 25 auxiliary qubits to significantly lift the MSC in Fig. 4, except for the setting of $m \to 1$. Compared with the strong coupling regime in Fig. 1, the greater number of auxiliary qubits ($N = 26$) have a more conspicuous influence on the enhancement of the MSC in Fig. 4. That is to say, the MSC is more sensitive to auxiliary qubits under the case of an initially weak coupling regime ($\lambda = 30, \gamma_0 = 5$), especially for a large number of auxiliary qubits.

As shown by Fig. 5, one can improve the MSC by introducing 5 or 25 auxiliary qubits both in ($r = 0.3, s = 0.2$) and ($r = -0.3, s = -0.2$) under different values of q. It is worthwhile emphasizing that the improvement effects of more auxiliary qubits ($N = 26$) on the MSC in Fig. 5 are significantly stronger than in the strong coupling regime in Fig. 2. Namely, one can use 25 auxiliary qubits to realize a greater increase in MSC for the scenario ($\lambda = 30, \gamma_0 = 5$).

In Fig. 6, the obvious oscillation phenomenon of the MSC disappears if we don't add auxiliary qubits in the reservoir, and the MSC monotonically decreases before it is frozen at a fixed value. If one couples 5 auxiliary qubits with the reservoir, the MSC can be sensibly augmented and can also be prematurely frozen at a fixed value. One can see from Fig. 6 that the 5 auxiliary qubits are poor at strengthening the MSC at smaller values of t. Of particular interest is that the introduction of 25 auxiliary qubits not only increases the MSC but also leads to oscillation of the MSC at smaller t. These results are different from those for the strong coupling regime in Fig. 3.

4. Conclusion

In summary, considering the strategy in which Alice and Bob share a two-qubit X state and the reservoir only directly disturbs Alice's atom and the GAD noise only affects Bob's atom, the MSC is examined by coupling auxiliary qubits with the reservoir. Our results reveal that auxiliary qubits can effectively enhance the MSC in the strong or weak coupling

regimes under various values of m, except for the choice of $m \to 1$. The MSC is frozen at a fixed value (namely, MSC is invariant) with growing q, and one can augment the fixed value of the MSC by coupling auxiliary qubits. The more auxiliary qubits that are introduced to the reservoir, the larger the fixed value obtained for the MSC. Under various values of t, the introduction of auxiliary qubits is responsible for the obvious increases in MSC in both the strong and weak coupling regimes, except for $t \to 0$. In the strong coupling regime, more auxiliary qubits can diminish the oscillation period of the MSC and also suppress the oscillation amplitude of the MSC under various values of t. In contrast, for the strategy of an initially weak coupling regime, the introduction of more auxiliary qubits can induce oscillation of the MSC in the case of $t \to 0$. In comparison with $(\lambda = 5, \gamma_0 = 30)$, a greater number of auxiliary qubits (such as $N = 26$) have a more conspicuous influence on the enhancement of the MSC under $(\lambda = 30, \gamma_0 = 5)$.

Acknowledgments

Project supported by the National Natural Science Foundation of China (Grant No. 12175001), the Key Project of Natural Science Research of West Anhui University (Grant No. WXZR202311), the Open Fund of Anhui Undergrowth Crop Intelligent Equipment Engineering Research Center (Grant No. AUCIEERC-2022-01), Anhui Undergrowth Crop Intelligent Equipment Engineering Research Center (Grant No. 2022AH010091), the Natural Science Research Key Project of Education Department of Anhui Province of China (Grant No. 2023AH052648), the University Synergy Innovation Program of Anhui Province (Grant No. GXXT-2021-026), and the Anhui Provincial Natural Science Foundation (Grant Nos. 2108085MA18 and 2008085MA20).

References

[1] Baumgratz T, Cramer M and Plenio M B 2014 *Phys. Rev. Lett.* **113** 140401
[2] Streltsov A, Adesso G and Plenio M B 2017 *Rev. Mod. Phys.* **89** 041003
[3] Hu M L, Hu X Y, Wang J C, Peng Y, Zhang Y R and Fan H 2018 *Phys. Rep.* **762-764** 1
[4] Napoli C, Bromley T R, Cianciaruso M, Piani M, Johnston N and Adesso G 2016 *Phys. Rev. Lett.* **116** 150502
[5] Zhang D J and Tong D M 2024 *Phys. Rev. Lett.* **133** 040202
[6] Du M M, Khan A S, Zhou Z Y and Zhang D J 2022 *Sci. China Phys. Mech. Astron.* **65** 100311
[7] Zhang D J, Wang Q H and Gong J 2019 *Phys. Rev. A* **99** 042104
[8] Zhang D J and Gong J 2020 *Phys. Rev. Research* **2** 023418
[9] Zhou Z Y, Qiu Z Y and Zhang D J 2024 *Phys. Rev. Res.* **6** L032048
[10] D J Zhang and D M Tong 2022 *npj Quantum Inf.* **8** 81
[11] Zhang D J, Wang Q H and Gong J 2019 *Phys. Rev. A* **100** 062121
[12] Girolami D 2014 *Phys. Rev. Lett.* **113** 170401
[13] Yu C S 2017 *Phys. Rev. A.* **95** 042337
[14] Winter A and Yang D 2016 *Phys. Rev. Lett.* **116** 120404
[15] Napoli C, Bromley T R, Cianciaruso M, Piani M, Johnston N and Adesso G 2016 *Phys. Rev. Lett.* **116** 150502
[16] Piani M, Cianciaruso M, Bromley T R, Napoli C, Johnston N and Adesso G 2016 *Phys. Rev. A* **93** 042107
[17] Mondal D, Pramanik T and Pati A K 2017 *Phys. Rev. A* **95** 010301
[18] Mondal D and Kaszlikowski D 2018 *Phys. Rev. A* **98** 052330
[19] Hu M L, Wang X M and Fan H 2018 *Phys. Rev. A* **98** 032317
[20] Hu M L and Fan H 2018 *Phys. Rev. A* **98** 022312
[21] Datta S and Majumdar A S 2018 *Phys. Rev. A* **98** 042311
[22] Ding Z Y, Yang H, Yuan H, Wang D, Yang J and Ye L 2019 *Phys. Rev. A* **100** 022308
[23] Ming F, Song X K, Ling J J, Ye L and Wang D 2020 *Eur. Phys. J. C* **80** 275
[24] Zhang D J, Liu C L, Yu X D and Tong D M 2018 *Phys. Rev. Lett.* **120** 170501
[25] Jevtic S, Pusey M, Jennings D and Rudolph T 2014 *Phys. Rev. Lett.* **113** 020402
[26] Milne A, Jevtic S, Jennings D, Wiseman H and Rudolph T 2014 *New J. Phys.* **16** 083017
[27] Milne A, Jennings D, Jevtic S and Rudolph T 2014 *Phys. Rev. A* **90** 024302
[28] Hu X Y and Fan H 2015 *Phys. Rev. A* **91** 022301
[29] Shi M J, Jiang F J, Sun C X and Du J F 2011 *New J. Phys.* **13** 073016
[30] Shi M J, Sun C X, Jiang F J, Yan X H and Du J F 2012 *Phys. Rev. A* **85** 064104
[31] Du M M, Zhang D J, Zhou Z Y and Tong D M 2021 *Phys. Rev. A.* **104** 012418
[32] Nguyen H C and Vu T 2016 *Phys. Rev. A* **94** 012114
[33] Jevtic S, Hall M J W, Anderson M R, Zwierz M and Wiseman H M 2015 *J. Opt. Soc. Am. B* **32** A40
[34] Quan Q, Zhu H J, Liu S Y, Fei S M, Fan H and Yang W L 2016 *Sci. Rep.* **6** 22025
[35] Nguyen H C and Vu T 2016 *Europhys. Lett.* **115** 10003
[36] McCloskey R, Ferraro A and Paternostro M 2017 *Phys. Rev. A* **95** 012320
[37] Caban P, Rembielinski J, Smolinski K A and Walczak Z 2017 *Quantum Inf. Process.* **16** 178
[38] Yang H, Xing L L, Du M M, Kong M, Zhang G and Ye L 2023 *Chin. Phys. B* **32** 100305
[39] Hu X Y, Milne A, Zhang B Y and Fan H 2016 *Sci. Rep.* **6** 19365
[40] Yang H, Du M M, Sun W Y, Ding Z Y, Wang D, Zhang C J and Ye L 2018 *Laser Phys. Lett.* **15** 125201
[41] Yang H, Ding Z Y, Sun W Y, Ming F, Fan X G, Wang D, Zhang C J and Ye L 2019 *Quantum Inf. Process.* **18** 299
[42] Maleki Y and Ahansaz B 2020 *Phys. Rev. A* **102** 020402
[43] Lan Y T and Hu M L 2023 *Results Phys.* **54** 107050
[44] Li H W, Fan Y H, Shen S T, Yan X J, Li X Y, Zhong W, Sheng Y B, Zhou L and Du M M 2024 *Eur. Phys. J. C* **84** 1241
[45] An B N 2013 *Phys. Lett. A* **377** 2520
[46] Behzadi N, Ahansaz B and Faizi E 2017 *Eur. Phys. J. D* **71** 280
[47] Faizi E and Ahansaz B 2019 *Phys. Scr.* **94** 115102
[48] Nourmandipour A, Tavassoly M K and Rafiee M 2016 *Phys. Rev. A* **93** 022327
[49] Nourmandipour A, Tavassoly M K and Bolorizadeh M A 2016 *J. Opt. Soc. Am. B* **33** 1723
[50] Stárek R, Mičuda M, Straka I, Nováková M, Dušek M, Ježek M, Fiurášek J and Filip R 2020 *New J. Phys.* **22** 093058
[51] Dias J, Wächtler C W, Nemoto K and Munro W J 2023 *Phys. Rev. Research* **5** 043295
[52] Götting N, Lohof F and Gies C 2023 *Phys. Rev. A* **108** 052427
[53] Kora Y, Zadeh-Haghighi H, Stewart T C, Heshami K and Simon C 2024 *Phys. Rev. A* **110** 042416
[54] Xie Y X and Sun Y H 2024 *Phys. Lett. A* **525** 129851
[55] Rastegar-Sedehi H R and Cruz C 2024 *Phys. Scr.* **99** 125936
[56] Huang Y Y 2024 *Results Phys.* **64** 107931
[57] Xu Q 2024 *Phys. Scr.* **99** 105128
[58] Liu Z Q, Liu J, Tan L and Liu W M 2024 *Phys. Rev. A* **110** 023707
[59] Yang H, Xing L L, Kong M, Zhang G and Ye L 2023 *Eur. Phys. J. C* **83** 966
[60] Hu M L and Xu X X 2022 *Ann. Phys. (Berlin)* **534** 2100412
[61] Nielsen M A and Chuang I L 2000 *Quantum Computation and Quantum Information (Cambridge University Press)*
[62] Wang S C, Yu Z W, Zou W J and Wang X B 2014 *Phys. Rev. A* **89** 022318
[63] Zou W J, Li Y H, Wang S C, Cao Y, Ren S C, Yin J, Peng S C, Wang X B and Pan J W 2017 *Phys. Rev. A* **95** 042342
[64] Ming F, Wang D, Huang A J, Sun W Y and Ye L 2018 *Quantum Inf. Process.* **17** 9
[65] Xu Z Y, Yang W L and Feng M 2012 *Phys. Rev. A* **86** 012113